

This is a repository copy of *Thylakoid localized bestrophin-like proteins are essential for the CO₂ concentrating mechanism of Chlamydomonas reinhardtii*.

White Rose Research Online URL for this paper:

<https://eprints.whiterose.ac.uk/148641/>

Version: Published Version

Article:

Mukherjee, Ananya, Lau, Chun Sing, Walker, Charlotte Elizabeth et al. (8 more authors) (2019) Thylakoid localized bestrophin-like proteins are essential for the CO₂ concentrating mechanism of Chlamydomonas reinhardtii. Proceedings of the National Academy of Sciences of the United States of America. pp. 16915-16920. ISSN 1091-6490

<https://doi.org/10.1073/pnas.1909706116>

Reuse

This article is distributed under the terms of the Creative Commons Attribution (CC BY) licence. This licence allows you to distribute, remix, tweak, and build upon the work, even commercially, as long as you credit the authors for the original work. More information and the full terms of the licence here:

<https://creativecommons.org/licenses/>

Takedown

If you consider content in White Rose Research Online to be in breach of UK law, please notify us by emailing eprints@whiterose.ac.uk including the URL of the record and the reason for the withdrawal request.

Thylakoid localized bestrophin-like proteins are essential for the CO₂ concentrating mechanism of *Chlamydomonas reinhardtii*

Ananya Mukherjee^a, Chun Sing Lau^b, Charlotte E. Walker^b, Ashwani K. Rai^a, Camille I. Prejean^a, Gary Yates^b, Thomas Emrich-Mills^b, Spencer G. Lemoine^a, David J. Vinyard^a, Luke C. M. Mackinder^{b,1}, and James V. Moroney^{a,1}

^aDepartment of Biological Sciences, Louisiana State University, Baton Rouge, LA 70803; and ^bDepartment of Biology, University of York, Heslington, York YO10 5DD, United Kingdom

Edited by Krishna K. Niyogi, Howard Hughes Medical Institute and University of California, Berkeley, CA, and approved July 15, 2019 (received for review June 7, 2019)

The green alga *Chlamydomonas reinhardtii* possesses a CO₂ concentrating mechanism (CCM) that helps in successful acclimation to low CO₂ conditions. Current models of the CCM postulate that a series of ion transporters bring HCO₃[−] from outside the cell to the thylakoid lumen, where the carbonic anhydrase 3 (CAH3) dehydrates accumulated HCO₃[−] to CO₂, raising the CO₂ concentration for Ribulose biphosphate carboxylase/oxygenase (Rubisco). Previously, HCO₃[−] transporters have been identified at both the plasma membrane and the chloroplast envelope, but the transporter thought to be on the thylakoid membrane has not been identified. Three paralogous genes (*BST1*, *BST2*, and *BST3*) belonging to the bestrophin family have been found to be up-regulated in low CO₂ conditions, and their expression is controlled by CIA5, a transcription factor that controls many CCM genes. YFP fusions demonstrate that all 3 proteins are located on the thylakoid membrane, and interactome studies indicate that they might associate with chloroplast CCM components. A single mutant defective in *BST3* has near-normal growth on low CO₂, indicating that the 3 bestrophin-like proteins may have redundant functions. Therefore, an RNA interference (RNAi) approach was adopted to reduce the expression of all 3 genes at once. RNAi mutants with reduced expression of *BST1–3* were unable to grow at low CO₂ concentrations, exhibited a reduced affinity to inorganic carbon (C_i) compared with the wild-type cells, and showed reduced C_i uptake. We propose that these bestrophin-like proteins are essential components of the CCM that deliver HCO₃[−] accumulated in the chloroplast stroma to CAH3 inside the thylakoid lumen.

Chlamydomonas | CO₂ concentrating mechanism | bicarbonate transport | photosynthesis | chloroplast thylakoid

Aquatic photosynthetic organisms, which account for close to 50% of the world's carbon fixation (1), face several challenges in carrying out efficient photosynthesis. Limitations include the slow diffusive rate of gases in water, fluctuations in pH, and the slow interconversion of inorganic carbon (C_i) forms. Thus, most aquatic autotrophs have developed an adaptation called the CO₂ concentrating mechanism (CCM) that increases the concentration of CO₂ around Ribulose biphosphate carboxylase/oxygenase (Rubisco) to increase its carboxylase activity. Aside from Rubisco's slow rate of catalysis, O₂ can compete with CO₂ for the active site of the enzyme, resulting in the wasteful process of photorespiration (2). Since CO₂ and O₂ are competitive substrates, the CCM reduces photorespiration and increases photosynthetic efficiency.

The CCM of the unicellular green alga *Chlamydomonas reinhardtii* (hereafter referred to as *Chlamydomonas*) has a number of bicarbonate (HCO₃[−]) transporters that help increase the HCO₃[−] concentration in the chloroplast stroma relative to the external HCO₃[−] concentration. These transporters are located on the plasma membrane (LCI1 and HLA3) as well as the chloroplast envelope (NAR1.2/LCIA). Loss of any one of these transporters reduces the ability of the cell to accumulate HCO₃[−] at high external pH (3, 4). In

addition, Rubisco is tightly packaged in a microcompartment of the chloroplast called the pyrenoid (5–7). Finally, carbonic anhydrase 3 (CAH3), located in the lumen of pyrenoid-traversing thylakoids, converts the accumulated HCO₃[−] to CO₂ near the site of Rubisco (8, 9), increasing photosynthetic and growth rates at otherwise growth-limiting CO₂ levels.

Carbonic anhydrases play an essential role in the *Chlamydomonas* CCM (10). The loss of CAH3 results in cells that cannot grow on air levels of CO₂, even though these mutants tend to overaccumulate HCO₃[−] (11). *Chlamydomonas* CCM models propose that mutants missing CAH3 accumulate the HCO₃[−] brought into the chloroplast by the transport proteins but cannot convert that HCO₃[−] to CO₂, the actual substrate of Rubisco (12, 13). These CCM models postulate that the pH gradient across the thylakoid membrane in the light helps drive the conversion of HCO₃[−] to CO₂. The apparent acid dissociation constant (pK_a) of the interconversion of HCO₃[−] and CO₂ is about 6.4, with the chloroplast stroma having a pH close to 8 in the light and the thylakoid lumen having a pH close to 5.7 under low CO₂ concentrations (14). Therefore, as HCO₃[−] is brought from the stroma to the thylakoid lumen, it goes from an environment favoring HCO₃[−] to one favoring CO₂. Therefore, the

Significance

Models of the CO₂ concentrating mechanism (CCM) of green algae and diatoms postulate that chloroplast CO₂ is generated from HCO₃[−] brought into the acidic thylakoid lumen and converted to CO₂ by specific thylakoid carbonic anhydrases. However, the identity of the transporter required for thylakoid HCO₃[−] uptake has remained elusive. In this work, 3 bestrophin-like proteins, *BST1–3*, located on the thylakoid membrane have been found to be essential to the CCM of *Chlamydomonas*. Reduction in expression of *BST1–3* markedly reduced the inorganic carbon affinity of the alga. These proteins are prime candidates to be thylakoid HCO₃[−] transporters, a critical currently missing step of the CCM required for future engineering efforts of the *Chlamydomonas* CCM into plants to improve photosynthesis.

Author contributions: A.M., C.S.L., C.E.W., D.J.V., L.C.M.M., and J.V.M. designed research; A.M., C.S.L., C.E.W., A.K.R., C.I.P., G.Y., T.E.-M., S.G.L., and J.V.M. performed research; A.M., C.S.L., C.E.W., A.K.R., L.C.M.M., and J.V.M. analyzed data; and A.M., C.S.L., C.E.W., D.J.V., L.C.M.M., and J.V.M. wrote the paper.

The authors declare no conflict of interest.

This article is a PNAS Direct Submission.

This open access article is distributed under [Creative Commons Attribution License 4.0 \(CC BY\)](#).

¹To whom correspondence may be addressed. Email: luke.mackinder@york.ac.uk or btmoro@lsu.edu.

This article contains supporting information online at www.pnas.org/lookup/suppl/doi:10.1073/pnas.1909706116/-DCSupplemental.

acidification of the thylakoid lumen is important to the functioning of the CCM.

The CCM models also proposed the presence of a thylakoid HCO_3^- transporter that brings in HCO_3^- from the stroma to the lumen for dehydration by CAH3 (12, 13). In a recent interactome study, the CCM complex LCIB/LCIC is shown to interact with the bestrophin-like proteins encoded by Cre16.g662600 and Cre16.g663450 (15). These proteins were also shown to interact with each other and another bestrophin-like protein encoded by Cre16.g663400 (15). All 3 genes were found to be up-regulated in low CO_2 conditions in a transcriptomic study showing they belonged to a cluster of genes that had increased expression in low CO_2 and were controlled by CIA5 (16). Bestrophins are typically chloride channels, including the *Arabidopsis* bestrophin-like protein AtVCCN1 (17). However, they have also been shown to transport a range of anions, with some showing high HCO_3^- permeability (18). The interactome study also putatively localizes these bestrophin-like proteins to the thylakoid membrane, which makes them promising candidates to be the thylakoid HCO_3^- transporter in the CCM of *Chlamydomonas*.

In the present study, we investigate the role of these 3 proteins using an RNA interference (RNAi) approach to knock down the expression of all 3 genes. This approach was feasible as the 3 genes are extremely similar at the DNA sequence level. Knockdown mutants with low expression of all 3 genes grow poorly in limiting CO_2 conditions, exhibit a poor affinity for external C_i , and have a severely reduced ability to accumulate HCO_3^- . This study sheds light on the intracellular location and function of these bestrophin-like proteins in the CCM of *Chlamydomonas*.

Results

***Chlamydomonas* Has 3 Very Similar Bestrophin-Like Proteins on the Thylakoid Membrane.** *BST1* (Cre16.g662600), *BST2* (Cre16.g663400), and *BST3* (Cre16.g663450) (collectively *BST1–3*) are paralogous bestrophin-like genes located within a 130-kilobase pair (kbp) region on the 16th chromosome of *Chlamydomonas*. Phylogenetic analyses revealed that bestrophin-like proteins are found in a diverse variety of photosynthetic organisms (Fig. 1), including vascular plants, nonvascular plants, and diatoms, with the homologs with the highest sequence identity to *BST1–3* found in algae. The amino acid sequences encoded by these genes were analyzed in TMHMM, which predicted that *BST1–3* are membrane proteins having 4 predicted transmembrane domains each. Further analysis using PredAlgo predicted that each *BST* protein had a chloroplast transit peptide and was likely to be a chloroplast membrane protein. *BST1* was annotated as a bestrophin-like protein in Phytozome (version 12.1), and *BST2* and *BST3* were previously reported as *LC111* by Fang et al. (16). An alignment between the 3 *Chlamydomonas* bestrophin-like proteins showed that the proteins are >80% identical to one another (SI Appendix, Fig. S1). There are 7 more genes annotated as encoding bestrophin-like proteins in the *Chlamydomonas* genome, but they share less than 50% identity to *BST1–3*. Sequence alignment of *BST1–3* with human Bestrophin 1 (BEST1) showed low sequence identity between BEST1 and *BST1–3* (21 to 23%; SI Appendix, Fig. S1). The most similar protein in terrestrial plants, the thylakoid localized AtVCCN1 protein of *Arabidopsis* (17), has approximately a 30% sequence identity with *BST1–3*. To further explore the potential structure and function of *BST1–3*, we did homology modeling using SWISS-MODEL (19). Structural studies show that human and *Klebsiella pneumoniae* bestrophins are pentameric, and modeling of *BST1* in a pentameric assembly is of high confidence (SI Appendix, Fig. S2A). The highest ranking template identified by SWISS-MODEL for *BST1–3* was *K. pneumoniae* bestrophin. *BST1–3* contain nonpolar residues along their selective pore that are conserved in proteins of the bestrophin family and are involved in anion transport (20) (SI Appendix, Fig. S2B). The entry pocket of *BST1* has a predominantly neutral/negative electrostatic potential, and the selective pore is positively charged, supporting the hypothesis that *BST1–3* transport negatively charged ions (19, 21) (SI Appendix, Fig. S2C and D), as does AtVCCN1 in *Arabidopsis* (17).

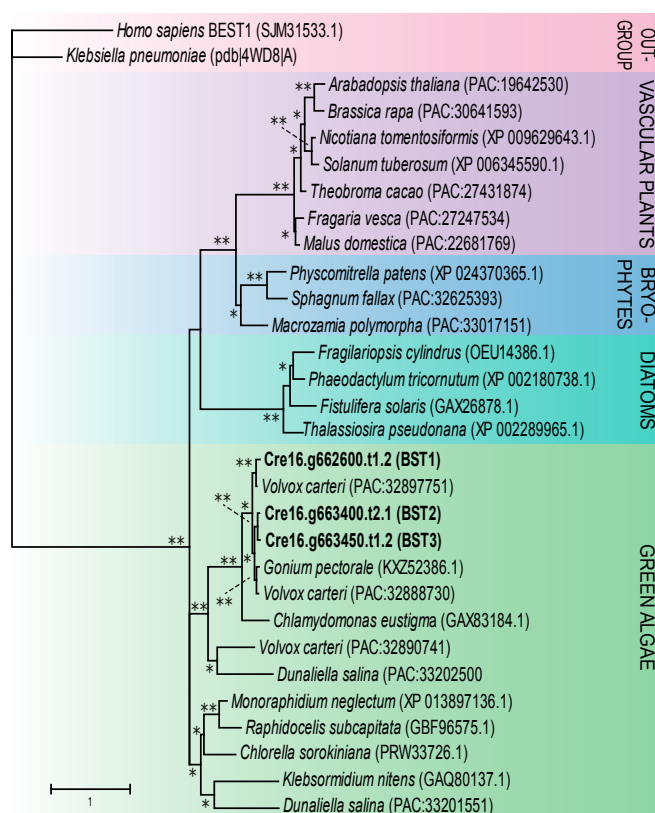


Fig. 1. Phylogenetic analysis of *Chlamydomonas* bestrophin-like proteins *BST1–3*. The evolutionary history of *Chlamydomonas* bestrophin-like proteins *BST1–3* was inferred by using the maximum likelihood method based on the Le and Gascuel (37) model with discrete Gamma distribution (5 categories) and 500 bootstrap replicates. The tree is drawn to scale, with branch lengths measured in the number of substitutions per site. *Bootstrap value ≥ 50 , **Bootstrap value ≥ 90 .

***BST1–3* Are Up-Regulated under Low CO_2 Growth Conditions and Localized to the Thylakoid.** Semiquantitative RT-PCR (Fig. 2A) was performed using complementary DNA isolated from strains D66 and *cia5* grown under high CO_2 or ambient CO_2 conditions. For this work, we have used 5% CO_2 (vol/vol) in air as high CO_2 , 0.04% as ambient CO_2 , and <0.02% as low CO_2 . D66 is the wild-type strain for these studies, and *cia5* is missing the CCM1 protein, which is required for the induction of the CCM in *Chlamydomonas* (22). This work demonstrated that all 3 *BST* genes were up-regulated under ambient CO_2 growth conditions in D66 and that this up-regulation was not observed in *cia5* (SI Appendix, Fig. S3A). In addition, the *cia5* mutant exhibited severely reduced expression of *BST1* and *BST3* under both CO_2 conditions, a transcriptional pattern observed with other CCM genes. *BST2* transcript levels in *cia5* cells showed reduced induction in ambient CO_2 when compared with D66 cells, where *BST2* transcript levels increase in ambient CO_2 conditions. A time course study of the expression of these 3 genes during induction of the CCM was done by transferring high CO_2 -grown cells to ambient CO_2 levels for 2 to 12 h (Fig. 2B and SI Appendix, Fig. S3B). All 3 genes had increased transcript levels within 2 h after the switch to low CO_2 , and these elevated levels of expression continued until at least 12 h after induction. *BST1* had a lower level of expression than *BST2* or *BST3* (Fig. 2).

To determine the localization of these 3 *BST*-like proteins in *Chlamydomonas*, fluorescent protein fusions were constructed linking Venus to the C terminus of each *BST* protein. All 3 *BST*-like proteins localized to the thylakoid membranes of the chloroplast (Fig. 3A), and this localization visibly extended into the thylakoid tubules of the pyrenoid (Fig. 3B). The localization

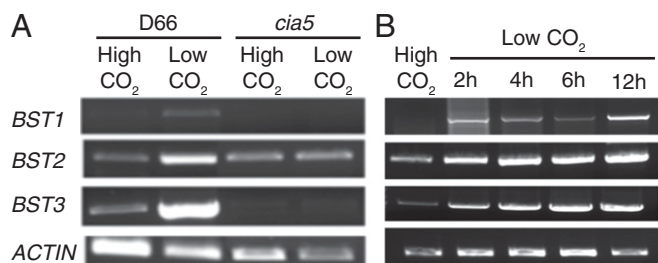


Fig. 2. Transcript analysis of *BST1-3*. (A) Semiquantitative RT-PCR showing *BST1-3* accumulation in ambient CO_2 (0.04% CO_2) vs. high CO_2 (5% [vol/vol] CO_2 in air) in D66 and *cia5* cells. (B) Semiquantitative RT-PCR time course showing the expression of *BST1-3* in complementary DNA obtained from high CO_2 (5% CO_2 [vol/vol] in air) and in cells switched to ambient CO_2 (0.04% CO_2) for the indicated times. Actin has been used as a loading control.

studies visually showed that *BST1*, *BST2*, and *BST3* were preferentially concentrated near the pyrenoid (Fig. 3B). To confirm that expression using the constitutive *PSAD* promoter was not affecting localization or pyrenoid periphery enrichment, we constructed a *BST3-Venus* line with the *BST3* gene under its native promoter. This line showed the same localization pattern as *BST3* under the constitutive *PSAD* promoter (Fig. 3C), and quantification of enrichment showed a 1.46-fold enrichment ($P < 0.01$, Student's paired *t* test) around the pyrenoid relative to the rest of the chloroplast. Thus, *BST1*, *BST2*, and *BST3* are thylakoid localized anion transporters enriched at the pyrenoid periphery that are expressed coordinately with the expression of other *Chlamydomonas* CCM proteins.

Reduction of *BST1-3* Expression Results in Cells that Grow Slowly under Low CO_2 Conditions. A *BST3* knockout (*bst3*) was obtained from the *Chlamydomonas* Library Project (CLiP) mutant collection (23) with a paromomycin insert in the last exon of the *bst3* gene (SI Appendix, Fig. S4A). The *BST3* transcript was not detected in *bst3* (SI Appendix, Fig. S4B), and the *BST3* protein was absent (SI Appendix, Fig. S4C). We observed a weak growth difference for this strain as compared with wild-type cells under ambient CO_2 (SI Appendix, Fig. S5A and B), but no clear phenotype on plates at pH 7 or pH 8.4 at 100 μmol of photons per $\text{m}^{-2}\cdot\text{s}^{-1}$ at low CO_2 (SI Appendix, Fig. S5C). However, there was no significant difference in C_i affinity between wild type and *bst3* grown at ambient CO_2 (SI Appendix, Fig. S5D), and C_i uptake by *bst3* was only slightly lower than wild type (SI Appendix, Fig. S5E and F). This led us to think that *BST1* or *BST2* function might be redundant with *BST3* and that the expression of all 3 genes must be reduced to determine their physiological role(s). Therefore, to elucidate the function of *BST1-3*, RNAi constructs complementary to regions of identity among *BST1-3* were designed (SI Appendix, Table S1). The D66 strain was transformed with these constructs, and colonies were kept at high CO_2 . Colonies were then screened for growth on high CO_2 versus low CO_2 , and *BST1-3* expression was quantified using RT-qPCR. Three independent colonies from 2 different transformations were chosen for further study and designated as *bsti-1*, *bsti-2*, and *bsti-3* (*BST* RNAi triple-knockdown lines 1, 2, and 3).

The growth of *bsti-1*, *bsti-2*, and *bsti-3* on high and low CO_2 was compared with D66 and the *CAH3* knockout mutant, *cia3* (Fig. 4A). In low CO_2 , *bsti-1* showed severely reduced growth that was further exacerbated at high pH, resembling the growth of *cia3* (Fig. 4A). The *bsti-2* and *bsti-3* also grew more slowly than wild-type cells, but better than *bsti-1*. However, at high CO_2 , the growth of all 3 strains was comparable to wild type. RT-qPCR showed that *bsti-1* had significantly reduced expression of *BST1*, *BST2*, and *BST3* compared with D66 (Fig. 4B), and *bsti-2* and *bsti-3* had a more moderate knockdown of expression of the 3 genes. To see if reduced transcript levels resulted in decreased protein abundance,

we checked *BST3* protein levels in the knockdown lines. All showed reduced levels relative to D66, although this was only significant for *bsti-2* and *bsti-3* ($P < 0.05$, Student's *t* test; SI Appendix, Fig. S6A). Thus, the *BSTs* are required for wild-type-like growth of *Chlamydomonas* under low CO_2 conditions.

Reduction of *BST1-3* Expression Also Results in Cells that Have a Reduced Capacity to Accumulate Inorganic Carbon. Two characteristics of algal cells with a CCM are a very high affinity for C_i and the ability to accumulate C_i to levels higher than can be obtained by diffusion. The *bsti-1*, *bsti-2*, and *bsti-3* acclimated to ambient CO_2 exhibited a lower affinity for C_i as judged by their measured C_i concentration needed for half-maximum oxygen evolution [$K_{1/2}(\text{C}_i)$] (Fig. 5). When grown at high CO_2 , *bsti1-3* and D66 exhibited similar C_i affinities (SI Appendix, Fig. S6B). These results indicate that the expression of *BST1-3* is required for optimal C_i affinity when cells are grown on ambient levels of CO_2 . At pH 8.4, the $K_{1/2}(\text{C}_i)$ values for *bsti1-3* are elevated in sharp contrast to a low $K_{1/2}(\text{C}_i)$ for D66 (Fig. 5A and B). At the higher pH of 8.4, the predominant C_i species in the medium would be HCO_3^- . Thus, the increased affinity of the cells for C_i reflects their ability to actively take up and utilize HCO_3^- . For *bsti-1*, where the expression of all 3 *BST* genes is between 60 and 90% reduced, there is a reduced C_i affinity at both pH 8.4 (Fig. 5A and B) and pH 7.8 (Fig. 5C and D). In contrast, *bsti3*, the mutant missing only *BST3*, the difference in C_i affinity with wild type (SI Appendix, Fig. S2B) is much smaller. Thus, we can conclude that *BST1-3* are necessary components of the CCM of *Chlamydomonas*.

C_i uptake activity was measured in D66, *bsti-1*, *bsti-2*, and *bsti-3* to evaluate the importance of *BST1-3* in accumulation and

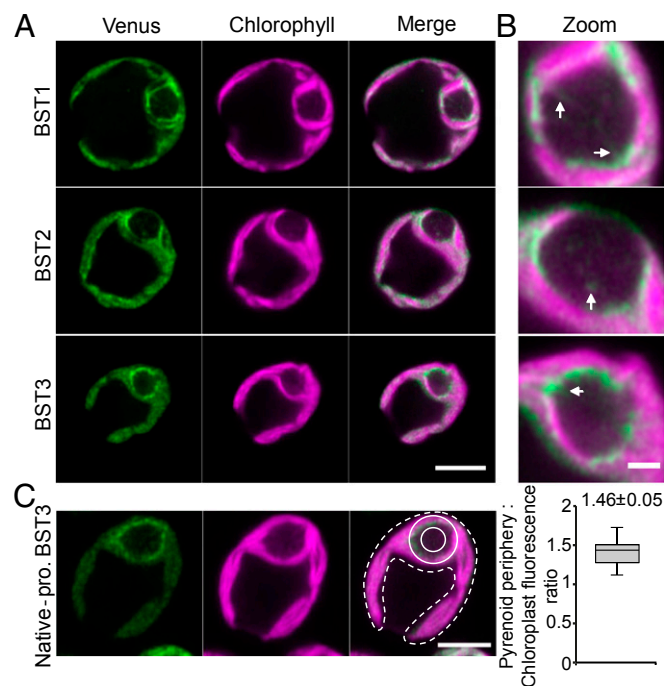


Fig. 3. Localization of *BST1-3*. (A) Confocal microscopy of *BST1-3* proteins fused with Venus (green) and driven by the constitutive *PSAD* promoter. Chlorophyll autofluorescence is shown in magenta. (Scale bar, 5 μm .) (B) Zoomed-in images of *BST1-3* pyrenoids shown in A. Arrows highlight where Venus fluorescence is seen overlapping with chlorophyll fluorescence in the pyrenoid matrix. (Scale bar, 1 μm .) (C) Localization and quantification of *BST3* distribution under its native promoter. The ratio of fluorescence intensity at the pyrenoid periphery (solid line region) and chloroplast (dotted line region) was quantified. The value above the plot denotes the mean \pm SE ($n = 23$). (Scale bar, 4 μm .)

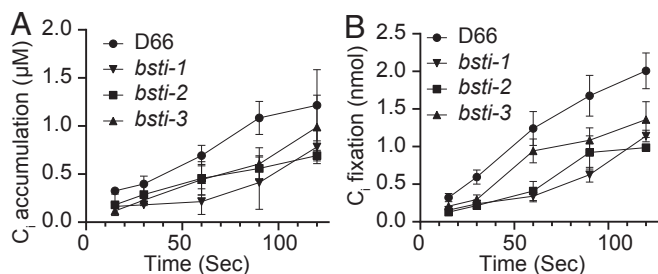


Fig. 6. C_i uptake of D66 and *bsti1-3*. C_i uptake and C_i accumulation were measured in D66 and *bsti1-3* using the silicone oil uptake method (Materials and Methods). Cells were grown in high CO_2 and then acclimated to ambient CO_2 for 12 h prior to the assays. Cells were harvested and depleted of endogenous C_i before running the assays. A time course of intracellular C_i accumulation (A) and CO_2 fixation (B) is shown for pH 8.4. Triplicate samples were run for each time point. The added $H^{14}CO_3^-$ concentration was 50 μM.

(16). Thus, the expression of the *BST1-3* genes is consistent with these proteins playing a role in the uptake and accumulation of C_i when *Chlamydomonas* is exposed to low CO_2 conditions.

An alternative hypothesis is that the 3 BST proteins have a function similar to AtVCCN1 (20) and are involved in Cl^- transport to regulate the pmf across the thylakoid. The presence of AtVCCN1 decreases pmf in *Arabidopsis*, but the presence of the 3 BST proteins increases pmf in *Chlamydomonas*. This result, in combination with our genetic and physiology data, suggests that the function of the BST proteins in *Chlamydomonas* is not the same as VCCN1 in *Arabidopsis*. A further understanding of this interconnection and the balancing/regulation of pmf within the context of the CCM is critical.

In *Chlamydomonas*, there seems to be a built-in redundancy of C_i transporter functions. For example, both LCI1 and HLA3 are present on the plasma membrane, and loss of only one of the proteins fails to cause an extreme growth phenotype at low CO_2 (3). However, when more than 1 transporter is knocked down, a significant change in C_i uptake and growth is observed (4, 5). *BST1-3* also appear to have redundant or overlapping functions. This is demonstrated in this study, as knocking out *BST3* by itself did not cause a drastic change in growth or reduction in C_i affinity at ambient levels of CO_2 (SI Appendix, Figs. S4 and S5). However, when the expression of all 3 genes is decreased in *bsti1-3*, cells could not grow at low CO_2 and C_i uptake was severely compromised. In addition, *BST1-3* transcript levels in the RNAi strains correlated to C_i affinity and C_i uptake, supporting their C_i transport role and functional redundancy. This redundancy likely explains why *BST1-3* were not identified in earlier mutant screens, as these screens typically knock out only 1 gene at a time. The 3 BST proteins do, however, have sequence differences, particularly at their C termini. Therefore, they might have specific (or slightly different) physiological roles that cannot be differentiated under the conditions employed in this present study.

Fig. 7 shows a refined model for the *Chlamydomonas* CCM, which now includes our proposed function for *BST1-3*. In this model, HLA3 and LCI1 transport HCO_3^- across the plasma membrane, bringing HCO_3^- into the cell (12, 13). At the chloroplast envelope, NAR1.2 (LCIA) transports HCO_3^- into the chloroplast stroma. Then, *BST1-3* on the thylakoid bring HCO_3^- into the thylakoid lumen, where CAH3 in the pyrenoid thylakoid tubules converts HCO_3^- to CO_2 to be fixed by Rubisco. Since *BST1-3* are found throughout the thylakoid, a potential futile cycle is possible. However, for the futile cycle to take place, CAH3 needs to be present and active in the thylakoid membranes away from the pyrenoid. There is published work that CAH3 is preferentially located and activated in the pyrenoid tubules under low (<0.02%) CO_2 conditions (8, 9). The location of *BST1-3* is also likely to be important in the recapture of CO_2 that is generated by the CCM (Fig. 7). Any CO_2 in the pyrenoid

not fixed by Rubisco has the potential to simply diffuse out of the cell (4, 27–29). The LCIB/C complex is thought to help recapture this CO_2 (27) by directionally driving CO_2 to HCO_3^- or by acting as a tightly regulated carbonic anhydrase (30) at the pyrenoid periphery (28). This is interesting because there are data supporting the interaction of LCIB/C with *BST1* and *BST3* (15). Our model adds *BST1-3* to this hypothesized recapture system (Fig. 7). Having *BST1-3* throughout the thylakoid (Fig. 3) would increase the surface area for the reuptake of HCO_3^- in the stroma. As such, we propose that the recapture of C_i is a 2-step process, with leaked CO_2 from the pyrenoid converted to HCO_3^- by LCIB/C and *BST1-3* transporting the HCO_3^- back into the thylakoid, creating an overall cyclic recapture mechanism. Loss of either *BST1-3* or LCIB/C results in cells that cannot accumulate C_i to normal levels, which agrees with experimental observations.

The discovery of CCM components on the thylakoid (*BST1-3*) and inside the thylakoid lumen (CAH3) also indicates how light energy may be used to energize the CCM. The apparent pK_a of the interconversion of HCO_3^- to CO_2 is about 6.4. The pH of the chloroplast stroma, thought to be near 8.0, is well above the pK_a , while the pH of the thylakoid lumen is thought to be close to 5.7 (14), below the pK_a . When HCO_3^- moves from the chloroplast stroma to the thylakoid lumen, it moves from an environment that favors HCO_3^- to one that favors CO_2 . This effectively allows the algal cells to increase the CO_2 concentration to levels higher than could be obtained by the action of carbonic anhydrase alone. Thus, a transthylakoid pH gradient is necessary for this proposed “ CO_2 pump,” and this pH gradient is set up by the photosystems and requires light. To date, all experimental data available indicate that light and the activity of the photosystems are required for the *Chlamydomonas* CCM to function. In fact, some of the earliest work in the field indicated that electron transport inhibitors and mutations that disrupt electron transport also inhibited the *Chlamydomonas* CCM (31, 32). One potential problem with this CO_2 pump model is that it would partially reduce the pmf across the thylakoid membrane, thus reducing ATP biosynthesis. However, it should be pointed out that only a single H^+ would be consumed per CO_2 generated, which is the

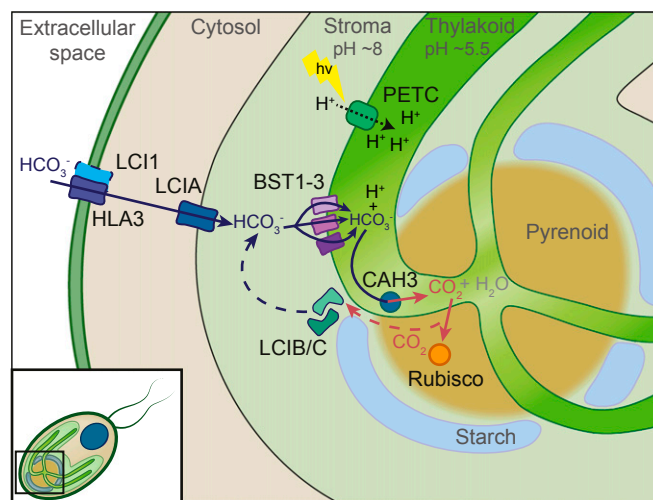


Fig. 7. Tentative model showing the proposed physiological role of *BST1-3* in the CCM of *Chlamydomonas*. Known transporters (LCI1, HLA3, and LCIA) are indicated on the plasma membrane and chloroplast, respectively. Solid line arrows indicate the movement of HCO_3^- into the thylakoid by *BST1-3*. Dashed lines indicate the proposed leakage-reducing pathway that involves recycling CO_2 by LCIB/C back to HCO_3^- . The dotted black line represents the light-driven establishment of a proton gradient across the thylakoid membrane by PSII and the cytochrome *b6f* complex of the photosynthetic electron transport chain (PETC).

equivalent of less than one-third of an ATP per CO₂ generated. This cost is far less than the 2 additional ATPs required for C₄ photosynthesis, and C₄ photosynthesis has been shown to be energetically competitive with C₃ photosynthesis once the costs of photorespiration are considered (33). In conclusion, BST1–3 are bestrophin-like, thylakoid localized membrane proteins that are synthesized in coordination with other CCM components, and their predicted structures fit well with functionally characterized bestrophins. As such, they are excellent candidates to be the HCO₃[−] transporters that not only bring HCO₃[−] into the thylakoid lumen for CO₂ generation but may also play a role in C_i recapture as well.

Materials and Methods

Cell Cultures, Growth, and Photosynthetic Assays. *C. reinhardtii* culture conditions were set according to the conditions used previously (34). The D66 strain (*nit2*[−], *cw15*, *mt*⁺) was obtained from Rogene Schnell (University of Arkansas, Fayetteville, AR), and CMJ030 (CC-4533; *cw15*, *mt*[−]) and *bst3* (BST3 knockout LMJ.RY0402.089365) were obtained from the CLiP collection at the *Chlamydomonas* culture collection (23, 35). For acclimation experiments, Tris-acetate-phosphate-grown cells were switched to minimal media and bubbled with high CO₂ (5% [vol/vol] CO₂ in air) to reach an optical density at 730 nm between 0.2 and 0.3 (~2 to 3 × 10⁶ cells per milliliter). This was followed by CCM induction when the cells were transferred to ambient CO₂ (0.04% CO₂) bubbling. For photosynthetic assays, cells acclimated to 5% or 0.04% CO₂ were resuspended in C_i-depleted buffer at pH 7.8 or pH 8.4, and O₂ evolution was measured at different C_i concentrations. K_{1/2}(C_i) was

calculated as the C_i concentration needed for the half-maximal rate of oxygen evolution.

Fluorescence Protein Tagging and Confocal Microscopy. The BST1–3 genes driven by the constitutive *PSAD* promoter were cloned as reported by Mackinder et al. (15). Briefly, the open reading frames of BST1–3 genes were PCR-amplified from genomic DNA and cloned into pLM005 with C-terminal Venus-3xFLAG and a *PSAD* promoter through Gibson assembly. BST3 driven by its native promoter was cloned using recombineering based on methods reported by Sarov et al. (36). Transformation of these genes into *Chlamydomonas* and selection of colonies are described in *SI Appendix, SI Materials and Methods*. Images were captured with a laser-scanning microscope (LSM880; Zeiss) equipped with an Airyscan module using a 63× objective with a 1.4 numerical aperture. Argon lasers at 514 nm and 561 nm were used for excitation of Venus and chlorophyll, respectively. Filters were set at 525 to 550 nm for the Venus emission and at 620 to 670 nm for chlorophyll emission.

Additional details of materials and methods are provided in *SI Appendix, SI Materials and Methods*.

ACKNOWLEDGMENTS. We thank the University of York Biosciences Technology Facility for confocal microscopy support. The project was funded by Biotechnology and Biological Sciences Research Council Grant BB/R001014/1 (to L.C.M.M.); Leverhulme Trust Grant RPG-2017-402 (to L.C.M.M. and C.E.V.); a University of York Biology Pump Priming award (to L.C.M.M.); and a subaward from the University of Illinois as part of the Realizing Increased Photosynthetic Efficiency project (to J.V.M.) funded by the Bill & Melinda Gates Foundation, Foundation for Food and Agriculture Research, and United Kingdom Aid.

1. P. Falkowski et al., The global carbon cycle: A test of our knowledge of earth as a system. *Science* **290**, 291–296 (2000).
2. H. Bauwe, M. Hagemann, A. R. Fernie, Photorespiration: Players, partners and origin. *Trends Plant Sci.* **15**, 330–336 (2010).
3. T. Yamano, E. Sato, H. Iguchi, Y. Fukuda, H. Fukuzawa, Characterization of co-operative bicarbonate uptake into chloroplast stroma in the green alga *Chlamydomonas reinhardtii*. *Proc. Natl. Acad. Sci. U.S.A.* **112**, 7315–7320 (2015).
4. Y. Wang, M. H. Spalding, Acclimation to very low CO₂: Contribution of limiting CO₂ inducible proteins, LCIB and LCIA, to inorganic carbon uptake in *Chlamydomonas reinhardtii*. *Plant Physiol.* **166**, 2040–2050 (2014).
5. O. N. Borkhsenius, C. B. Mason, J. V. Moroney, The intracellular localization of ribulose-1,5-bisphosphate carboxylase/oxygenase in *chlamydomonas reinhardtii*. *Plant Physiol.* **116**, 1585–1591 (1998).
6. L. C. Mackinder et al., A repeat protein links Rubisco to form the eukaryotic carbon-concentrating organelle. *Proc. Natl. Acad. Sci. U.S.A.* **113**, 5958–5963 (2016).
7. M. Rawat, M. C. Henk, L. L. Lavigne, J. V. Moroney, *Chlamydomonas reinhardtii* mutants without ribulose-1,5-bisphosphate carboxylase-oxygenase lack a detectable pyrenoid. *Planta* **198**, 263–270 (1996).
8. A. Blanco-Rivero, T. Shutova, M. J. Román, A. Villarejo, F. Martinez, Phosphorylation controls the localization and activation of the luminal carbonic anhydrase in *Chlamydomonas reinhardtii*. *PLoS One* **7**, e49063 (2012).
9. M. Mitra et al., The carbonic anhydrase gene families of *Chlamydomonas reinhardtii*. *Can. J. Bot.* **83**, 780–795 (2005).
10. J. V. Moroney et al., The carbonic anhydrase isoforms of *Chlamydomonas reinhardtii*: Intracellular location, expression, and physiological roles. *Photosynth. Res.* **109**, 133–149 (2011).
11. J. Karlsson et al., A novel alpha-type carbonic anhydrase associated with the thylakoid membrane in *Chlamydomonas reinhardtii* is required for growth at ambient CO₂. *EMBO J.* **17**, 1208–1216 (1998).
12. J. V. Moroney, R. A. Ynalvez, Proposed carbon dioxide concentrating mechanism in *Chlamydomonas reinhardtii*. *Eukaryot. Cell* **6**, 1251–1259 (2007).
13. M. H. Spalding, Microalgal carbon-dioxide-concentrating mechanisms: *Chlamydomonas* inorganic carbon transporters. *J. Exp. Bot.* **59**, 1463–1473 (2008).
14. K. Takizawa, J. A. Cruz, A. Kanazawa, D. M. Kramer, The thylakoid proton motive force in vivo. Quantitative, non-invasive probes, energetics, and regulatory consequences of light-induced pmf. *Biochim. Biophys. Acta* **1767**, 1233–1244 (2007).
15. L. C. M. Mackinder et al., A spatial interactome reveals the protein organization of the algal CO₂-concentrating mechanism. *Cell* **171**, 133–147 e14 (2017).
16. W. Fang et al., Transcriptome-wide changes in *Chlamydomonas reinhardtii* gene expression regulated by carbon dioxide and the CO₂-concentrating mechanism regulator CIA5/CCM1. *Plant Cell* **24**, 1876–1893 (2012).
17. A. Herdean et al., A voltage-dependent chloride channel fine-tunes photosynthesis in plants. *Nat. Commun.* **7**, 11654 (2016).
18. Z. Qu, H. C. Hartzell, Bestrophin Cl[−] channels are highly permeable to HCO₃[−]. *Am. J. Physiol. Cell Physiol.* **294**, C1371–C1377 (2008).
19. A. Waterhouse et al., SWISS-MODEL: Homology modelling of protein structures and complexes. *Nucleic Acids Res.* **46**, W296–W303 (2018).
20. Z. Qu, L. T. Chien, Y. Cui, H. C. Hartzell, The anion-selective pore of the bestrophins, a family of chloride channels associated with retinal degeneration. *J. Neurosci.* **26**, 5411–5419 (2006).
21. V. Kane Dickson, L. Pedi, S. B. Long, Structure and insights into the function of a Ca²⁺-activated Cl[−] channel. *Nature* **516**, 213–218 (2014).
22. H. Fukuzawa et al., Ccm1, a regulatory gene controlling the induction of a carbon-concentrating mechanism in *Chlamydomonas reinhardtii* by sensing CO₂ availability. *Proc. Natl. Acad. Sci. U.S.A.* **98**, 5347–5352 (2001).
23. X. Li et al., An indexed, mapped mutant library enables reverse genetics studies of biological processes in *Chlamydomonas reinhardtii*. *Plant Cell* **28**, 367–387 (2016).
24. S. Kikutani et al., Thylakoid luminal θ -carbonic anhydrase critical for growth and photosynthesis in the marine diatom *Phaeodactylum tricornutum*. *Proc. Natl. Acad. Sci. U.S.A.* **113**, 9828–9833 (2016).
25. J. V. Moroney et al., Isolation and characterization of a mutant of *Chlamydomonas reinhardtii* deficient in the CO₂ concentrating mechanism. *Plant Physiol.* **89**, 897–903 (1989).
26. S. Jin et al., Structural insights into the LCIB protein family reveals a new group of β -carbonic anhydrases. *Proc. Natl. Acad. Sci. U.S.A.* **113**, 14716–14721 (2016).
27. D. Duanmu, Y. Wang, M. H. Spalding, Thylakoid lumen carbonic anhydrase (CAH3) mutation suppresses air-Dier phenotype of LCIB mutant in *Chlamydomonas reinhardtii*. *Plant Physiol.* **149**, 929–937 (2009).
28. T. Yamano et al., Light and low-CO₂-dependent LCIB-LCIC complex localization in the chloroplast supports the carbon-concentrating mechanism in *Chlamydomonas reinhardtii*. *Plant Cell Physiol.* **51**, 1453–1468 (2010).
29. A. Kaplan, L. Reinhold, CO₂ concentrating mechanisms in photosynthetic microorganisms. *Annu. Rev. Plant Physiol. Plant Mol. Biol.* **50**, 539–570 (1999).
30. L. C. M. Mackinder, The *Chlamydomonas* CO₂-concentrating mechanism and its potential for engineering photosynthesis in plants. *New Phytol.* **217**, 54–61 (2018).
31. M. R. Badger, A. Kaplan, J. A. Berry, Internal inorganic carbon pool of *Chlamydomonas reinhardtii*: Evidence for a carbon dioxide-concentrating mechanism. *Plant Physiol.* **66**, 407–413 (1980).
32. M. H. Spalding, R. J. Spreitzer, W. L. Ogren, Carbonic anhydrase-deficient mutant of *Chlamydomonas reinhardtii* requires elevated carbon dioxide concentration for photoautotrophic growth. *Plant Physiol.* **73**, 268–272 (1983).
33. J. V. Moroney, N. Jungnick, R. J. Dimario, D. J. Longstreth, Photorespiration and carbon concentrating mechanisms: Two adaptations to high O₂, low CO₂ conditions. *Photosynth. Res.* **117**, 121–131 (2013).
34. Y. Ma, S. V. Pollock, Y. Xiao, K. Cunnusamy, J. V. Moroney, Identification of a novel gene, CIA6, required for normal pyrenoid formation in *Chlamydomonas reinhardtii*. *Plant Physiol.* **156**, 884–896 (2011).
35. R. Zhang et al., High-throughput genotyping of green algal mutants reveals random distribution of mutagenic insertion sites and endonucleolytic cleavage of transforming DNA. *Plant Cell* **26**, 1398–1409 (2014).
36. M. Sarov et al., A recombineering pipeline for functional genomics applied to *Caenorhabditis elegans*. *Nat. Methods* **3**, 839–844 (2006).
37. S. Q. Le, O. Gascuel, An improved general amino acid replacement matrix. *Mol. Biol. Evol.* **25**, 1307–1320 (2008).